

Laser ranging: a critical review of usual techniques for distance measurement

Markus-Christian Amann

Technische Universität München
Walter Schottky Institut
D-85748 Garching, Am Coulombwall
Germany

Thierry Bosch

Marc Lescure

ENSEEIH-Laboratoire d'Electronique
2 Rue Charles Camichel
F 31071 Toulouse
France
E-mail: bosch@len7.enseeiht.fr

Risto Myllylä

University of Oulu
Department of Electrical Engineering and
Infotech Oulu
P.O. Box 4500
90014 Oulu
Finland

Marc Rioux

National Research Council, Canada
Institute for Information Technology
Visual Information Technology
Ottawa, Canada, K1A 0R6

Abstract. We review some usual laser range finding techniques for industrial applications. After outlining the basic principles of triangulation and time of flight [pulsed, phase-shift and frequency modulated continuous wave (FMCW)], we discuss their respective fundamental limitations. Selected examples of traditional and new applications are also briefly presented. © 2001 Society of Photo-Optical Instrumentation Engineers.
[DOI: 10.1117/1.1330700]

Subject terms: distance measurement; laser ranging; triangulation; three-dimensional vision; laser radar.

Paper DDM-10 received July 24, 2000; accepted for publication July 24, 2000.

1 Introduction

Absolute distance measuring devices are at an important evolutionary stage in industrial countries in terms of applications such as nondestructive testing, reverse engineering predictive maintenance or virtual reality. They have the potential to improve the productivity of firms or the quality of manufactured products. In particular, noncontact distance measurements of rough targets are of great interests for many industrial applications.

The basic principle of active noncontact range-finding devices is to project a signal (radio, ultrasonic or optical) onto an object and to process the reflected or scattered signal to determine the distance. If a high resolution range-finder is needed, an optical source must be chosen because radio and ultrasonic waves cannot be focused adequately. In addition to absolute distance measurement, laser range-finding devices are traditionally used for 3-D vision, dimensional control, positioning or level control.

Optical distance measurement methods can technically be put into three categories: interferometry, time-of-flight and triangulation methods.¹ Considerable progress has been achieved during recent years by understanding the basic physical and information theoretical principles of range sensing. It appears that the advance in the design of lasers, integrated optics devices, emitter and receiver electronics will lead to further interesting developments.

In this paper, some laser range-finding techniques for industrial applications are briefly presented: triangulation, pulsed time-of-flight, phase-shift measurement and frequency-modulated continuous wave (FMCW) modulation. All these approaches are still further developed because the choice of the technique to be used depends mainly on the required application. Moreover, each of them presents limitations, which are discussed here.

2 Optical Triangulation for 3-D Digitizing

The desire to capture shape by optical means dates back to the beginning of photography.² In the 1860s François Villème invented a process known as photosculpture, which used 24 cameras. Profiles of the subject to be reproduced were taken on photographic plates, projected onto a screen (using the magic lantern), and transferred to a piece of clay using a pantograph.

Commercial applications developed rapidly; studios opened in Paris, London, and New York. They stayed in operation from 1863 to 1867, when it was realized that the photosculpture process was not more economical than the traditional way of doing sculpture. In any case, the process still required a lot of human intervention. Indeed, the photosculpture process supplied only 24 profiles, which were used to rough down the piece of clay, leaving a large amount of manual work to be done to finish the sculpture. A professional sculptor was needed and the photosculpture

process required quite an investment in terms of cameras, projection and reproduction systems, and skilled labor to operate them. It is only with the advent of computers that the process has regained substantial interest, more than 100 years later.

The surface shape of objects can be imaged and digitized using the following basic components: a light source to define a specific pixel(s), such as an encoding-decoding process (e.g., triangulation, fringe and pattern projections, and time of flight), a sensing device composed of a collecting lens and a photodetector that converts light energy to electrical signal, an analog-to-digital converter, and finally a computer to process, display, and store the raw data.³

The following reviews the basic concepts behind optical triangulation for 3-D digitizing applications. It emphasizes the critical elements of optimal design and the limitations related to the use of coherent light. It is shown, for example, that speckle noise is a fundamental limit for the position sensing of laser spot centroid. This has an impact on the choice of the position sensor geometry. Design guidelines are also presented.

2.1 Light Source

Conventional light sources can and are used for optical triangulation, but laser sources have unique advantages for 3-D imaging. One of these is brightness, which cannot be obtained by an incoherent emitter. Another is the spatial coherence that enables the laser beam to “stay in focus” when projected on the scene. Nevertheless, this property is limited by the law of diffraction, which is written here as the propagation (along the z axis) of Gaussian laser beams.

$$\omega(z) = \omega_0 \left[1 + \left(\frac{\lambda z}{\pi \omega_0^2} \right)^2 \right]^{1/2}, \quad (1)$$

and, defining depth of field D_f using the Rayleigh criterion gives:

$$D_f = 2 \pi \omega_0^2 / \lambda, \quad (2)$$

which shows that the depth of field D_f is larger when the laser wavelength λ is small (toward the blue) and/or when the laser beam spot size ω_0 is large. A detailed analysis is given in Ref. 4.

Figure 1 shows a graph of the preceding equation when a pixel (voxel) is sampled every ω_0 in the X , Y , and Z directions. On the horizontal axis are the physical dimensions of the “volume of view” along the X , Y , and Z directions, assuming that the volume of view is a cube. Vertically are the number of pixels (voxels) resolved along the three-axis. A few typical laser wavelengths are shown. This graph can be used as a guide when designing an optical system for imaging shapes. It shows the maximum number of pixels (in terms of information transfer) that can be extracted from a specific volume. As an example, for a cube that is 50 cm on a side, one has access to more than 2000 resolved spots in each direction axis X , Y , and Z using visible wavelength laser light, which correspond to a cubic element (voxel) of 200 μm on the surface of the illuminated object.

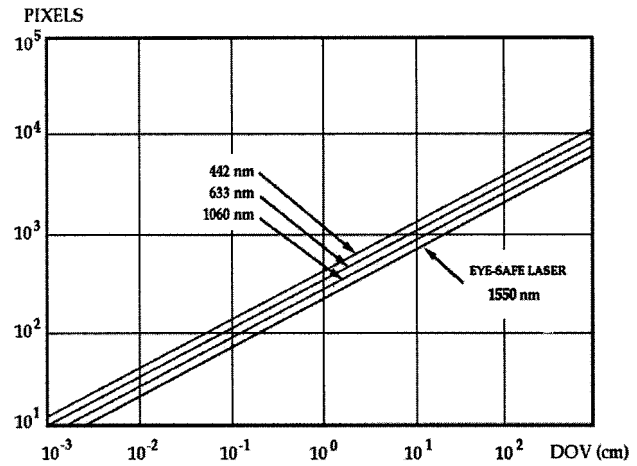


Fig. 1 Image resolution of a diffraction-limited optical 3-D laser scanner for four typical laser wavelengths.

2.2 Optical Triangulation Geometry

On scattering, the spatial coherence of the laser light is lost, which means that the depth of field used at the projection can be useful only if the lens aperture is closed down at the collection. Otherwise the focused laser spot is imaged as a blurred disk of light on the photodetector. A solution to this problem is to modify the conventional imaging geometry to conform to the Scheimpflug condition.

Essentially this geometry enables the photodetector surface to “stay in focus” with the projected laser light. Its construction is very simple when the focal planes of the lens are used. Indeed, it is known that a point on the projection axis located at f (point 1) will be imaged at infinity (Fig. 2). Consequently the inclination angle of the photodetector is defined by drawing a line between that point and the principal point of the collecting lens (line 1). Similarly, on the other side of the lens, one knows that a point at infinity will be imaged at a distance f from the lens. The inclination and position of the photodetector are then obtained by constructing a line (line 2) parallel to line 1 passing through the point 2.

2.3 Fundamental Limits

Sampling the shape along the X and the Y axes is usually done in a straightforward manner [time or space interval, depending on the geometry of the photodetector(s)]. Sam-

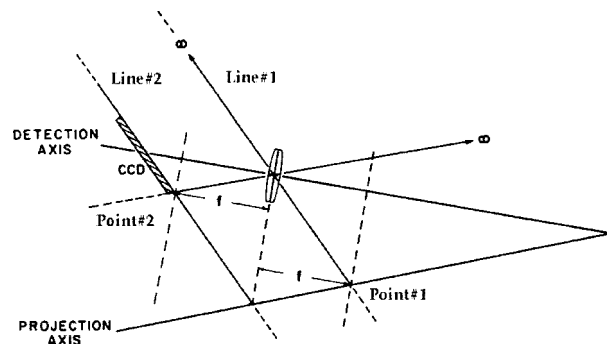


Fig. 2 Geometric construction of the Scheimpflug condition.

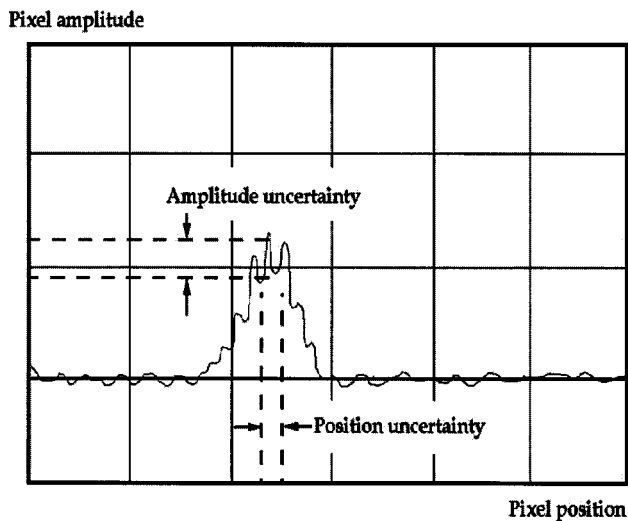


Fig. 3 Speckle noise limits the position sensing resolution.

pling along the third dimension (Z axis) often requires image pattern centroid location and interpolation. This is where coherence shows its limitation. Indeed, because of the coherent nature of the laser projection, the imaged laser spot on the photodetector(s) is corrupted with speckle noise. Here again, the geometry of the optical system and the wavelength of the light are the parameters.

Figure 3 shows how speckle noise adds to the uncertainty of an imaged laser spot. The origin of the modulation observed in the profile is related to the scattering of a pure wavelength when diffusion occurs at the surface of the object.

Within the projected laser spot, each scatterer can be regarded as a coherent emitter, and because there are many of them within the area of illumination the resulting image is the coherent sum of spatially incoherent sources. The result is a random modulation multiplying the expected smooth light profile. In Ref. 5, the relationship between the geometrical parameters is established as:

$$\sigma^2 = \lambda^2 f_0^2 / 2\pi (\phi \cos \beta)^2, \quad (3)$$

where σ^2 is the position variance, λ the wavelength of the laser light, f_0 is the lens-CCD distance on the optical axis, ϕ is the aperture of the collecting lens, and β is the Scheimpflug angle.

When typical values are given for each parameter, the centroid uncertainty is found to be of the order of a few micrometers, and more interesting, the physical dimensions of the photosensor elements have no effect on that limit. Consequently, the larger the photosensors, the better are the performances of the 3-D digitizer in terms of sensitivity, speed, and depth of view. In practice, using wider photosensor elements means that the interpolation is done over a wider dynamic range. As an example, if the speckle noise limits is at $2 \mu\text{m}$ and the photosensor width is at $16 \mu\text{m}$, one requires only 5 bits of numerical interpolation. On the other hand, if the photosensor width is $50 \mu\text{m}$, 7 bits of interpolation are required. Notice that at least 2 bits are added to the ratio to reduce quantization (or numerical) noise to a negligible level.

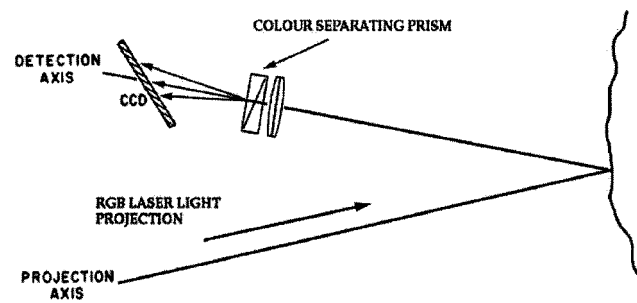


Fig. 4 Geometry for simultaneous recording of shapes and colors.

2.4 Color

A very simple way to add color to a digitized shape is illustrated in Fig. 4, which is essentially the same optical triangulation geometry as in Fig. 2, with two modifications. Here the single wavelength laser is replaced by a RGB laser or a multiwavelength laser consisting of arbitrary colors in arbitrary numbers. As an example, an Ar-Kr gas laser emits simultaneously more than 10 colors in the visible part of the spectrum. Each can be used to make color measurements. This is the modification at the projection level.

The second modification is made at the collection level. A prism (or a wedge) is used to disperse the multiwavelength laser beam into multiple beams, each having an amplitude related to the "color" of the illuminated point on the surface of the object. An interesting feature of this geometry is that the shape and color are digitized simultaneously, enabling a perfect registration of geometric and color data.

2.5 Conclusion

Digitizing shapes requires careful design consideration. For all active approaches including optical triangulation, the most critical element in order to achieve high-resolution imaging is the projection system, not the collecting system. In fact, in some cases it is found that optimum performances are obtained where the photosensor elements are of larger sizes. This is quite the opposite of the current trend in conventional 2-D imaging. Applications of 3-D digitizing cover a wide spectrum from industrial design, manufacturing, simulation, inspection, and visual communication.

3 Laser Pulse Time-of-Flight Distance Measurement

3.1 Introduction

The laser pulse time-of-flight (TOF) distance measuring technique was originally used in military and surveying applications. It refers to the time it takes for a pulse of energy to travel from its transmitter to an observed object and then back to the receiver (t_d). If light is used as energy source, the relevant parameter involved in range counting is the speed of light (roughly $c = 30 \text{ cm/ns}$). A TOF system measures the round trip time between a light pulse emission and the return of the pulse echo resulting from its reflectance off an object. Using elementary physics, distance is determined by multiplying the velocity of light by the time light takes to travel the distance. In this case, the measured time is representative of traveling twice the distance and must,

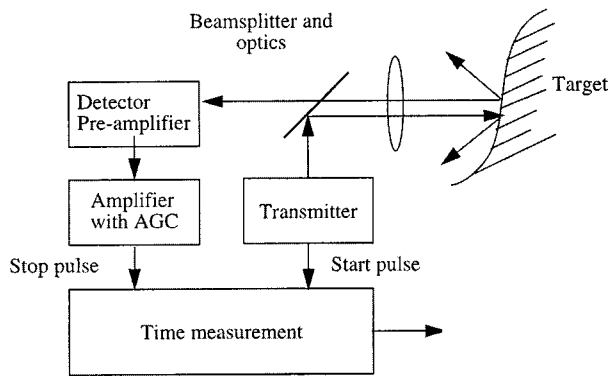


Fig. 5 Block diagram of TOF laser range finder.

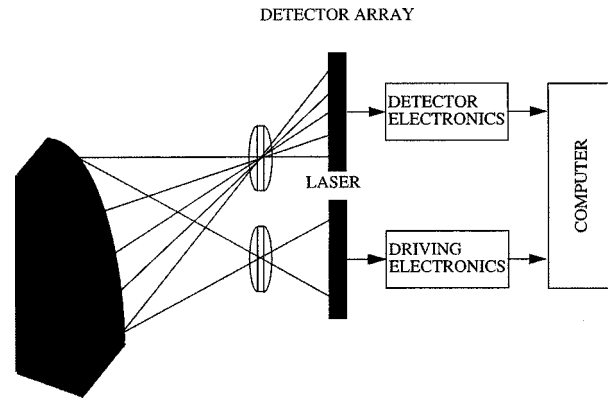


Fig. 6 Schematic of focal plane scanning.

therefore, be reduced by half to give the actual range to the target. To obtain 1 mm accuracy, the accuracy of the time interval measurement should be 6.7 ps.

Since a single pulse is adequate for the unequivocal determination of distance with centimeter precision and accuracy depends only weakly on distance, this method is particularly appropriate, for example, in applications involving distances longer than 1 m, applications where reflectors are not used and fast measurement applications such as scanning. In addition, averaging enables millimeter or even sub-millimeter precision to be achieved. The advantage of the TOF system arises from the direct nature of its sensing as both the transmitted and returned signals follow essentially the same direct path to an object and back to the receiver.

Some new applications such as sensors in robotics, autonomous vehicles and rendezvous and docking, along with anticollision and proximity sensors and sensors used in protecting an area in front of a machine demand limitations on instrument size, mass and power consumption. To achieve these goals, the basic building blocks of a TOF range finder have to be realized in the form of high-performance integrated circuits. Bosch and Lescuré provide an excellent review of absolute distance measurement in one of the SPIE Milestone volumes.¹

3.2 Constructions

A pulsed TOF distance measuring device consists of a laser transmitter emitting pulses with a duration of 5 to 50 ns, a receiver channel including a *p-i-n* or an avalanche photodiode, amplifiers, an automatic gain control (AGC) and timing discriminators. The emitted light pulse (start pulse) triggers the time interval measurement unit, and the reflected light pulse (stop pulse) stops it. The distance to the target is proportional to the time interval. A block diagram of a laser range finder is shown in Fig. 5.

The selection of laser type depends on the intended measurement range and the required speed. For long distances (up to several kilometers), a Nd:YAG laser can be used, giving peak powers extending to the megawatt level. Low-priced pulsed laser diodes [single heterostructure (SH) or double heterostructure (DH)-type], capable of producing peak powers of tens of watts, enable measuring distances up to a few hundreds of meters—or even longer using coherent summing. The repetition frequency of YAG lasers is low, whereas laser diodes can be used at rates of tens of kilohertz, the DH-type may even reach the megahertz level.

In 3-D measurements, the laser range finder is equipped with angle encoders to enable the definition of the coordinates of the measurement point. Scanning is mechanical and is carried out manually or automatically. In some applications, manual scanning is adequate but for time-critical purposes a servo system is required to increase the measurement rate. Basic techniques include scanning either the measuring head or only the measuring beam by means of galvanometer-driven mirrors.

Focal plane scanning can be used instead of a narrow laser beam, which scans a surface mechanically, point by point. This enables a range map to be obtained without mechanical beam scanning. The result is highly improved 3-D mapping performance, particularly with respect to measuring time, at considerably reduced mechanical complexity and thus reduced size and power requirements. The principle of focal plane scanning is presented in Fig. 6.

The laser beam illuminates the total field of view on the surface. A target's surface is viewed using matrices of separate detectors. Each detector covers its own fraction of the field of view illuminated by the laser. Detector signals are analyzed in the time domain, and distances to particular points are calculated on the basis of time interval measurements. The system can simultaneously measure distances to several directions without any moving parts.⁶

3.3 Timing Jitter and Walk, Nonlinearity and Drift

The main sources of inaccuracy in laser rangefinders are noise-generated timing jitter, walk, nonlinearity and drift. Typical noise sources include noise generated by the electronics, shot noise caused by the background radiation-induced current and shot noise created by the noise of the signal current. Jitter in timing determines mainly the precision of the range measurement. The amount of timing jitter is proportional to noise amplitude [root mean square (rms)] and inversely proportional to the slope of the timing pulse at the moment of timing (du/dt). A single-shot resolution of 1 cm can typically be achieved with a good signal (SNR=100) using the 100 MHz bandwidth of the receiver channel. However, precision deteriorates as the distance increases and the pulse amplitude decreases proportional to the square of the distance.⁷ Pulse amplitude and shape variations create timing error in the time-pickoff circuit and that error is called walk error. Jitter and walk in leading edge timing are shown in Fig. 7.

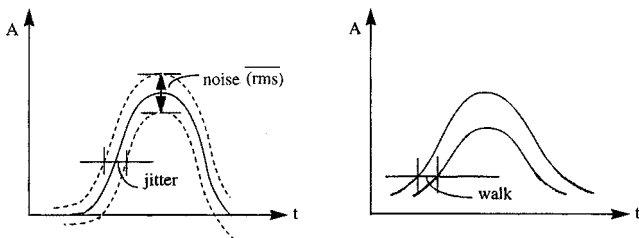


Fig. 7 Timing jitter and walk.

The time discriminator is a very important part of a precision time measurement system. The task of the discriminator is to observe time information from the electric pulse of the detector preamplifier and to produce a triggering signal at the right instant. The choice of time derivation method depends on the desired time resolution, counting rate and required dynamic range of the pulse. Commonly used principles in discriminator design include leading edge timing (constant amplitude), zero crossing timing (derivation), first moment timing (integration), and constant fraction timing. Constant fraction discrimination (CFD) compensates with idealized pulse shapes for walk caused by both amplitude and risetime and is commonly used in the TOF measuring units of laser range finders.

The principle behind the operation of CFD is the search for an instant in the pulse when its height bears a constant ratio to pulse amplitude. The occurrence of this point produces a triggering pulse. The constant fraction instant can be examined with a high gain differential emitter-coupled logic (ECL) comparator, which amplifies the difference of the attenuated and the delayed pulses.⁸ CFD compensates for walk caused by amplitude and rise time, but not for walk caused by unlinear shape variations. Zero crossing and first moment timing compensate for amplitude variations, while leading edge timing fails to compensate for any variation described.

The transmitter, gain-control and time-interval measurement units are also critical for the accuracy of the system. The transmitter should be able to produce a stable laser pulse shape. This may call for the temperature stabilization of the diode. The dynamic phenomena of the laser diodes, relaxation oscillations, should also be considered when designing the pulsing scheme as they may easily lead to significant changes in laser pulse shape.

Gain control is needed to adjust the dynamics of the timing pulse to that of the timing discriminator. The amount of control needed depends on the measurement range, construction of the optics and reflectivity variations of the object. An adjustable optical attenuator at the receiver optics can be used to realize gain control. The advantage of this method over electrical gain control is its delay stability over a wide control range. Recently, the dynamic range of electronic gain control methods has increased quite remarkably.⁹

The time interval between the start and stop pulses is measured with the time-to-digital converter (TDC), which is a fast, accurate and stable time-interval measuring device that uses, e.g., a digital counting technique together with an analog or digital interpolation method.¹⁰ The single shot resolution of the TDC is typically better than the noise generated timing jitter.

The final precision of the distance measurement can be greatly improved by averaging, with the improvement being proportional to the square root of the number of results averaged. Thus, by averaging 100 successive measurements, the final resolution can be improved to the millimeter level, the corresponding measurement time being 1 ms with a pulsing rate of 100 kHz, for instance.

If the statistical error is averaged to a negligible level, the accuracy of the system is defined by its systematic errors such as nonlinearity in the time interval measurement scale and drift. A careful design of the system can reduce these errors to the millimeter level.

3.4 New Applications and Development Trends

Several new applications for the transit time measurement of laser pulses are currently being developed to supplement traditional ones. A promising method involves using the path length of light pulses in human tissue, pulp and paper or optical fiber as a sensor principle. In this context, the term photon migration is often used to describe the propagation of light in scattering media like human tissue. In turbid media, photons take a number of different paths thereby broadening short light pulses. The use of TOF techniques for imaging soft tissues (optical tomography) is being actively investigated by many researchers today for applications such as breast cancer diagnosis and imaging the oxygenation state of the brain in newborn infants.¹¹ From the point of view of the paper industry, one of the most important properties of graphic paper is the interaction of light and paper structure. One method of obtaining a more detailed understanding of the propagation of light in paper and pulp is the high-resolution measurement of the delay light pulses suffer as they pass through a sheet of paper or a sample of pulp.¹² As for composite materials, optical fibers can be embedded in them during the manufacturing process. Calculations are then based on the fact that the TOF of the light pulse in a fiber is a function of the length and refractive index of the fiber, which are affected by stress, temperature and pressure.¹³

Commercial applications in the civilian sector place several demands on laser-based devices. First, the so-called class 1 laser condition (eye-safety) that limits the peak power of the laser to a few watts should be fulfilled. However, the reliable detection of low-reflectance or high-temperature targets requires a sufficiently high optical peak power. The use of picosecond pulses helps to overcome the eye-safety problem, but at the cost of a receiver with high bandwidth. Shorter pulses also give better precision.¹⁴ Other highly desirable qualities of the range finder include cost-effectiveness. The size, weight and power consumption of the device should be reduced to increase its potential application range. These goals can be achieved using full custom application-specific integrated circuits (ASIC). A long-term vision could be to realize the TOF range finder as a component-like microsystem where all the basic elements (laser diode, photodetector, receiver channel and time interval measurement electronics) are located on a single encapsulated hybrid circuit.

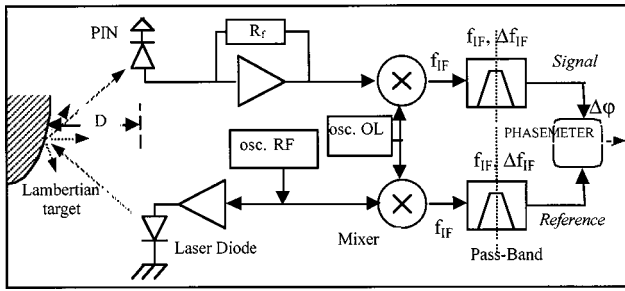


Fig. 8 Block diagram of a phase-shift laser rangefinder using a heterodyne technique.

4 Principle and Limitations of a Laser Phase-Shift Range Finder

4.1 Introduction

The principle of a laser phase-shift range finder is described in this section. Heterodyne technique gives a narrow bandwidth amplification which improves the SNR. The limitations such as high level of the photoelectric signal, intermediate frequency drift and electrical crosstalk are discussed.

4.2 Physical Principle of a Phase-Shift Rangefinder

In a phase-shift rangefinder, the optical power is modulated with a constant frequency. The basic operating scheme of the device is shown in Fig. 8. A sine wave of frequency f_{rf} generated by the main oscillator modulates the dc current of the laser diode. After reflection from the target, a photodiode collects a part of the laser beam. Measurement of the distance D is deduced from the phase shift $\Delta\varphi = 2\pi f_{rf}\Delta t$ between the photoelectric current and the modulated emitted signal:

$$D = \frac{1}{2} c \frac{\Delta\varphi}{2\pi f_{rf}}, \quad (4)$$

where c is the speed of light in free space and Δt is the TOF.

When $\Delta\varphi = 2\pi$, the unambiguous distance measurement is limited to $\Lambda = cf_{rf}/2$ (for example, $\Lambda = 9$ m with $f_{rf} = 16.66$ MHz). To ameliorate the accuracy of this setup, the phase shift is not directly measured at the working high frequency but at an intermediate frequency $f_{if} = |f_{rf} - f_{ol}|$ using a heterodyne technique that preserves the phase shift versus distance. The signals of the two mixers outputs are filtered by a passband circuit tuned on f_{if} and with a Δf_{if} bandwidth.

4.3 Received Signal Power

When the target area is as large as the area illuminated by the transmitter, the received signal power P_R is given by the relationship:

$$P_R = T_T T_R \frac{\rho_d}{\pi} P_0 \cos \theta \frac{A_R}{D^2}, \quad (5)$$

where

P_0 = power output of the laser diode

T_T = collection and transmission efficiency of transmitter

T_R = transmission of the receiver optics

ρ_d = Lambertian reflection coefficient of the target

θ = laser beam incident angle on the target

A_R = area of receiver lenses.

Only, the Lambertian component is used for the calculation of the photoelectric signal; the specular component is ignored in Eq. (5). As a matter of fact, the term $\rho_d P_0 / \pi$ is the power intensity (in watts per steradian) reflected perpendicular to the target surface.

For some representative construction materials (such as standard printing white paper, unpainted wood, unpolished coating, satin-like coating) the values of ρ_d are between 0.6 and 0.7 for a wavelength $\lambda = 820$ nm (Ref. 15). With $\lambda = 950$ nm, values can vary from 0.4 to 0.8 (Ref. 16).

4.4 Error Analysis

4.4.1 High levels on the rf channel

The power budget shows that the ratio P_R/P_0 may vary with a factor greater than 1000 if the distance D varies for example from 1 to 10 m. Thus, when the photoelectric signal amplitude varies with a factor 1000, the phase-shift error $\delta\varphi$ introduced by this variation must be less than 0.1 deg for an error distance measurement δD of 2.5 mm. But, with large amplitude of the useful signal, distortion and clipping introduce phase-shift errors. To avoid this error, the first solution is the defocusing of the photodiode, so that it receives less light when measured distances are small. A second solution is increasing the feedback of the mixer to avoid distortion and clipping.¹⁷

4.4.2 Intermediate frequency drift

With a low-power laser diode, a narrow bandwidth amplification improves the SNR. For a white noise at the input, the output of a passband second-order filter presents a noise-equivalent bandwidth B_n given by the relationship¹⁸:

$$B_n = (\pi/2) \Delta f_{if}. \quad (6)$$

Thus, the rms noise of the useful signal is proportional to the square root of the bandwidth Δf_{if} . Because of symmetry, it can be supposed that the frequency drift δf_{rf} or δf_{ol} of one oscillator balances the drift of the other one. No error is present if the two intermediate frequency filters are identical on reference channel and signal channel. But if the value of the bandwidth is too narrow, we must take into account the device mismatch effects introduced in intermediate frequency tuned circuits by the frequency drifts of f_{rf} and f_{ol} . For example, for Rauch filter structure, the quality factor $Q = f_{if}/\Delta f_{if}$ and the tuned frequency f_{if} mismatches are imposed by the presence of capacitance mismatches. With $f_{rf} = 16.66$ MHz, $\Delta f_{if} = 200$ Hz, assuming a capacitance mismatch of 1%, to achieve a phase-shift error

smaller than $\delta\varphi = 0.1$ deg (distance error $\delta D = 2.5$ mm), the required stability of the two main oscillators is $\delta f_{\text{rf}}/f_{\text{rf}} \approx 3.5 \times 10^{-7}$.

However, to guarantee the resolution, the best method consists of keeping the value of the intermediate frequency constant by a phase-locked loop technique. In Refs. 19 and 20, 100 m distance measurement to a retroreflector is obtained (i.e., with a good SNR) with errors of less than 50 μm . The stable $f_{\text{rf}} = 1.5$ GHz modulating frequency is generated from the 15th harmonic of a 100 MHz output of a Rubidium atomic clock.

4.4.3 Influence of the crosstalk

Electrical crosstalk between the transmitter and the receiver produces another important error. When the photoelectric signal and the modulation current of the laser diode have the same frequency f_{rf} , the synchronous leakage v_{crosst} , arising from the modulation current source, is superimposed on the working photoelectric signal v_{ph} . The two signals are added vectorially. The transimpedance amplifier associated with the photodiode must be shielded to exclude undesired external signals. However, because the influence of the crosstalk cannot be totally removed with shielding techniques, different methods have been proposed. To remove the effects of this field leakage, the gain switch of a laser diode is used as a light comb generator, and an avalanche photodiode (APD) selects the second harmonic of the photoelectric signal.²¹ Another method, based on the use of a Pockels cell, has been proposed to obtain a measured signal at a frequency that is a multiple of the modulation frequency, although its implementation is still rather difficult.²²

The crosstalk errors at the modulation frequency f_{rf} determine the minimum signal-to-induction ratio necessary to obtain a given accuracy. For example, to limit the maximum error phase shift $\delta\varphi$ to 0.1 deg, the amplitude ratio of the photoelectric signal on the leakage signal must be 600 (55 dB). Because the induced signal is “masked” by the electrical noise, the SNR must be higher than 55 dB. This condition is difficult to satisfy when the frequency modulation f_{rf} of a low-power laser diode is higher than 10 MHz. The maximum distance measurement error δD_{max} is independent from the modulation frequency and increases with the square of the distance, in accordance with Eq. (5). Because the photoelectric current and crosstalk are added vectorially, a periodic error is obtained versus distance D . In this way, this error can be compensated.²³

To determine a rough estimation of the crosstalk between the driver laser and the photodiode, a model of fictitious sources of perturbation at the input of the transimpedance amplifier has been proposed.²⁴ The coupling is represented by the mutual capacitance and the mutual inductance. These models show the advantage of using an APD. Indeed, the gain of the primary photoelectric current occurs inside the semiconductor crystal itself, and it can be assumed that the crosstalk becomes superimposed on the output signal only when the signal has been amplified. But, as APD areas are small, this gives a small field of view of the receiver. For 3-D vision, if only the laser beam is deflected by micromirrors, a large field of view of the receiver is necessary, when no scanning mirrors are used in the

receiver channel. A large *p-i-n* photodiode surface gives such a field of view. So, the large photodiode capacitance increases the time constant at the input of signal channel, that reduces the bandwidth and/or the phase margin of the transimpedance amplifier. One solution is to compensate the photodiode capacitance by a tuned circuit. This technique is possible because the phase-shift range finder is working at one frequency f_{rf} only.

4.5 Conclusion

Distance measurement by the phase-shift technique is a good method to obtain a resolution of some millimeters in 1 to 20 m ranges with noncooperative targets. For cooperative targets (cube corner), the resolution can be better than 50 μm , with high-frequency modulation. Because the photoelectric current is a sine wave, a photodiode with a large area can be used to achieve a wide angle of the field of view. In this way, it is possible to scan the laser beam by micromirrors, enabling compactness and low cost of future 3-D vision system.

5 FMCW Optical Radar

5.1 Introduction

Optical distance measurement with the FMCW technique has been used in various applications such as noncontact surface profiling, fiber optic sensing, reflectometry, positioning and tomography. The interest in the FMCW technique is due to the large dynamic range and the high resolution, particularly at short range sensing. Because of the recent progress in the area of laser diode technology, high-performance FMCW ranging systems can currently be realized with electronically tunable laser diodes.^{25–29} In this paper, we therefore describe the operation principle of the FMCW technique and discuss the system performance achievable with laser diodes.

5.2 Principle

The principal setup of an optical FMCW radar system is illustrated in Fig. 9. The optical power from a frequency modulated laser diode, the instantaneous frequency of which is periodically shifted by Δf , is used as probing signal as shown in Fig. 10(a).

The periodic and linear frequency chirp may practically be performed by applying a saw-tooth bias current to the modulator section of the wavelength-tunable laser diode. The laser output passes an optical isolator to avoid deteriorations of the laser frequency by reflections and is then sent simultaneously to the object and the reference mirror, and the reflected signals are then superimposed in a square law detector diode. Owing to the detection process that is proportional to power, i.e., the amplitude squared, both signals are mixed in the detector and the main ac component of the electrical output is at the frequency difference f_{if} of the two optical signals. The detector output is fed into an amplifier-limiter so that unintentional amplitude modulation is suppressed. Finally, the intermediate frequency f_{if} of the reflected signals is measured with a frequency counter. Due to the square law mixing process the amplitude of the detector output at f_{if} is proportional to the amplitudes (not the powers) of the object signal and the reference, respec-

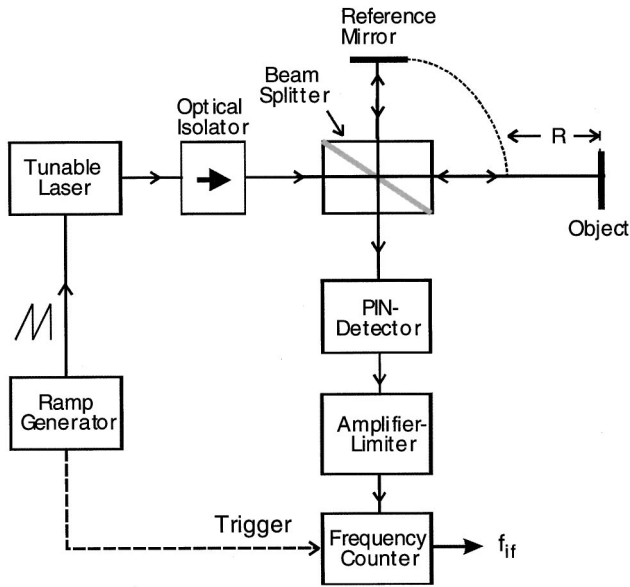


Fig. 9 Principle setup of an FMCW optical radar system using a tunable laser diode as light source.

tively. Accordingly, the dynamic range of the FMCW technique is twice as large than that of the pulse radar technique, where the electrical signal is proportional to the object signal power.

The range difference between object and reference mirror R , which is the relevant quantity to be determined, is proportional to f_{if} as indicated in Fig. 10(a). Since the round-trip delay time τ of the object signal is given as

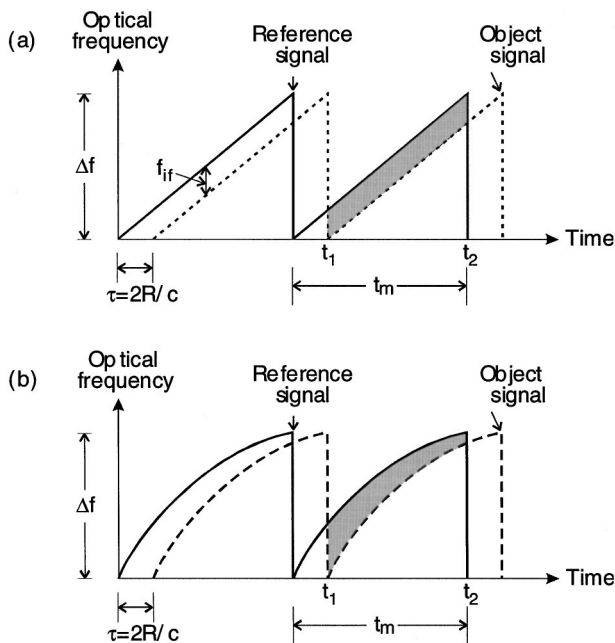


Fig. 10 Instantaneous optical frequencies versus time of the object and reference mirror optical signals (a) in case of a linear optical frequency ramp, the intermediate frequency f_{if} is constant between t_1 and t_2 and (b) in case of a nonlinear optical frequency ramp, a chirping intermediate frequency occurs.

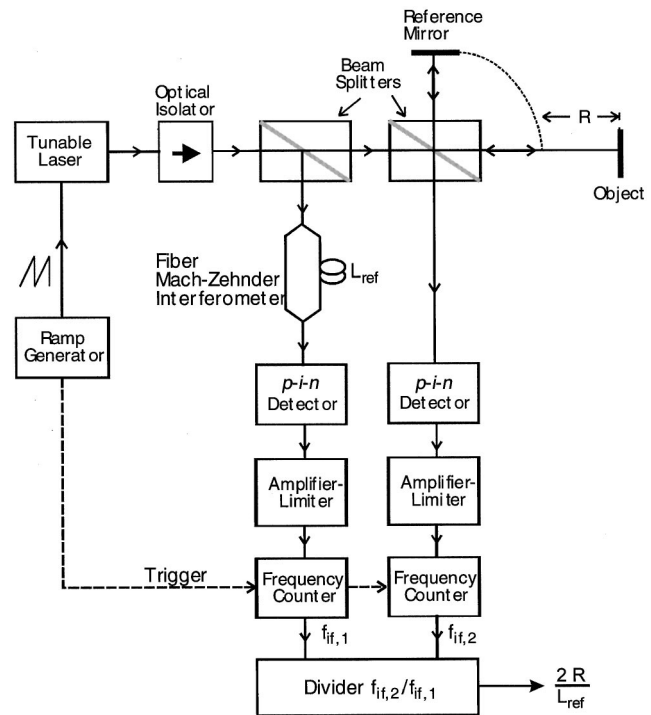


Fig. 11 Schematic setup of an improved FMCW optical radar system with a reference line to eliminate the effect of a nonlinear optical frequency ramp.

$$\tau = 2R/c, \tag{7}$$

where c is the light velocity, the intermediate frequency amounts to

$$f_{if} = \Delta f \tau / t_m = 2 \Delta f R / c t_m, \tag{8}$$

where t_m denotes the ramp period, which is typically of the order 0.1 to 1 ms. Accordingly, the distance sensing is done by an electric frequency measurement (usually in the kilohertz regime), while in the case of the more popular pulse radar, the delay time is measured directly. Since the ramp period can be chosen arbitrarily, the FMCW radar can determine τ values in the picosecond range, according to millimeter distances R , by simply performing a frequency measurement in the kilohertz regime. Consequently, no high-speed electronic is required to determine delay times even in the subpicosecond range, according to micrometer distances R occurring, e.g., in the automated inspection of printed boards.

5.3 Limitations

Unfortunately, the frequency modulation response of a laser diode is, in general, nonuniform against the modulation frequency, so that a linear optical frequency sweep cannot be realized by a linear modulation of the control current. In addition, the frequency versus control current characteristic is also in general nonlinear. As a consequence, deviations from the linear ramp as shown in Fig. 10(b) usually occur that, in turn, lead to a variation of the intermediate frequency f_{if} as shown schematically in Fig. 11. While the total phase difference ϕ as indicated by the shaded areas in

Figs. 10(a) and 10(b) is still proportional to τ and the distance R as long as $\tau \ll t_m$, the variation of f_{if} during each ramp increases the total intermediate frequency bandwidth and, consequently, the noise level that finally limits the accuracy. A usual technique to eliminate the effect of the nonlinear frequency ramp is to use simultaneously a reference line, as shown in Fig. 11, so that the ratio of distance R and the length of the reference line L_{ref} is independent of the linearity of the frequency ramp.³⁰ Various schemes have been presented to linearize the optical frequency sweep of the laser diodes, that commonly utilize a reference delay line similar to Fig. 11 to determine the variations of the intermediate frequency $f_{if,1}$. By means of an electrical feedback path the control current ramp to the laser is adjusted such that $f_{if,1}$ is kept constant.³¹ As a consequence, the current ramp deviates from linearity in such a way that the relevant instantaneous optical frequency versus time characteristic becomes linearized according to Fig. 10(a).

The maximal measurable distance of an FMCW laser diode system is finally limited by the coherence length of the laser diode. The finite value of the latter, which typically is of the order of several tens of meters is a consequence of the laser diode phase noise that also determines the spectral linewidth. Correspondingly, laser diodes with narrow linewidths within the frequency sweep range are best suited for the measurement of longer distances. Recently, however, it was shown that this limitation can be overcome by application of a frequency-shifted feedback laser and range measurements up to 18 km were reported.³²

Also the ultimate limitation of the measurement accuracy is due to the phase noise of the laser diode.^{33,34} Again, frequency-modulated laser diodes with narrow spectral linewidth are in general preferable for highly accurate range measurements. However, it should be noted that the low-frequency phase noise occurring in the f_{if} frequency range is relevant. Strictly speaking, therefore, in case of nonwhite phase noise the laser linewidth represents not a useful quantity to estimate the relevant phase noise. This particularly holds for the widely continuously tunable laser diodes that exhibit large Δf values of the order of several hundred gigahertz with the correspondingly large sensitivity. Experimentally, high resolution in the submicrometer regime has been demonstrated with diode laser FMCW ranging systems.²⁸ Using widely continuously tunable laser diodes with Δf of 500 GHz, a spectral linewidth of 25 MHz, and a repetition period t_m of 10 μ s, the one-shot relative accuracies for distances of 1 m and 1 cm, respectively, amount³⁵ to 4.3×10^{-5} and 2.7×10^{-4} . These results clearly prove the high performance of this technique for the accurate and fast measurement of short distances and, considering the large modulation bandwidth of laser diodes, make this technique also well suited for 3-D viewing systems.

6 Conclusion

Usual laser distance measuring techniques were briefly reported. This paper presented the basic principles of triangulation and TOF (pulsed, phase-shift, and FMCW) and some related applications. It also emphasized their fundamental limitations and proposed solutions to improve their performances in terms of accuracy, sensitivity and cost.

This brief review of laser range-finding techniques holds out the promise of an exciting future for traditional and new industrial applications.

References

1. T. Bosch and M. Lescure, Eds., *Selected Papers on Laser Distance Measurement*, SPIE Milestone Series, Vol. MS 115, SPIE Optical Engineering Press, Bellingham, WA (1995).
2. B. Newhall, "Photosculpture," *Image* 7(5), 100–105 (1958).
3. M. Rioux, F. Blais, J.-A. Beraldin, and P. Boulanger, "Range imaging sensors development at NRC laboratories," in *Proc. IEEE Workshop on Interpretation of 3D Scenes*, pp. 154–160, Austin, TX (1989).
4. M. Rioux, G. Bechthold, D. Taylor, and M. Duggan, "Design of a large depth of view three-dimensional camera for robot vision," *Opt. Eng.* 26(12), 1245–1250 (1987).
5. R. Baribeau and M. Rioux, "Influence of speckle on laser range finders," *Appl. Opt.* 30(20), 2873–2878 (1991).
6. R. Myllylä, J. Marszalec, J. Kostamovaara, A. Mäntyniemi, and G.-J. Ulbrich, "Imaging distance measurements using TOF lidar," *J. Opt.* 29, 188–193 (1998).
7. K. Määttä, J. Kostamovaara, and R. Myllylä, "Profiling of hot surfaces by pulsed time-of-flight laser range finder techniques," *Appl. Opt.* 32(27), 5334–5347 (1993).
8. M. R. Maier and P. Sperr, "On the construction of a fast constant fraction trigger with integrated circuits and application to various phototubes," *Nucl. Instrum. Methods* 87, 13–18 (1970).
9. T. Ruotsalainen, P. Palojärvi, and J. Kostamovaara, "A current-mode gain-control scheme with constant bandwidth and propagation delay for transimpedance preamplifier," *IEEE J. Solid-State Circuits* 34(2), 253–258 (1999).
10. E. Räisänen-Ruotsalainen, T. Rahkonen, and J. Kostamovaara, "Integrated time-to-digital converters based on interpolation," *J. Analog Integr. Circ. Signal Process.* 15(1), 49–57 (1998).
11. A. J. Joblin, "Method of calculating the image resolution of a near-infrared time-of-flight tissue-imaging system," *Appl. Opt.* 35(4), 752–757 (1996).
12. J. Carlsson, P. Hellentin, A. Malmqvist, W. Persson, and C.-G. Wahlström, "Time-resolved studies of light propagation in paper," *Appl. Opt.* 34(9), 1528–1535 (1995).
13. H. Lahtinen, M. Jurvakainen, P. Pramila, H. Tabell, M. Kusevic, O. Hormi, V. Lyöri, M. Heikkinen, R. Myllylä, P. Suopajarvi, and H. Kopola, "Utilisation of optical fibre measurement techniques in determination of residual stresses of composites," *Proc. SPIE* 3746, 526–529 (1999).
14. G. Kompa, "Powerful picosecond pulsed laser radar with micrometer ranging resolution," in *Proc. 26th Eur. Microwave Conf.*, pp. 147–152 (1996).
15. T. Bosch and M. Lescure, "Experimental determination of the useful reflection coefficient of non-cooperative targets for a time-of-flight laser rangefinder," *Opt. Rev.* 2(B04), 289–291 (1995).
16. D. Nitzan, A. Brain, and R. Duda, "The measurement and use of registered reflectance and range data in scene analysis," *Proc. IEEE* 65(2), 206–220 (1977).
17. G. Perchet, M. Lescure, and Th. Bosch, "Errors analysis of phase-shift laser range finder with high level signal," *Sens. Actuators A* 62(1–3), 534–538 (1997).
18. E. Cherry and D. Hooper, *Amplifying Devices and Low-Pass Amplifier Design*, Wiley, New York (1968).
19. J. M. Payne, D. Parker, and R. F. Bradley, "Rangefinder with fast multiple range capability," *Rev. Sci. Instrum.* 63(6), 3311–3316 (1992).
20. M. A. Goldman, R. E. Creager, D. H. Parker, and J. M. Payne, "Rangefinder metrology for the Green bank telescope," in *Proc. EOS Topical Meeting on Optoelectronic Distance/Displacement Measurements and Applications*, (1997).
21. K. Seta and T. Oh'ishi, "Distance measurement using a pulse train emitted from a laser diode," *Jpn. J. Appl. Phys., Part 2* 26, L1690–L1692 (1987).
22. M. Lescure, T. Bosch, and A. Dziadowiec, "An electro-optical frequency doubling method to remove electrical noise in laser range finder," *IEEE Trans. Instrum. Meas.* 40, 1046–1047 (1991).
23. R. Müller, H. Wölfelschneider, M. Kublin, and H. P. Anderer, "Application limits of optical distance measuring based on the phase detection technique," in *Proc. EOS Topical Meeting on Optoelectronic Distance/Displacement Measurements and Applications*, (1997).
24. Th. Bosch and M. Lescure, "Error analysis of 1–10 m laser phase-shift rangefinder," *IEEE Trans. Instrum. Meas.* 46(6), 1224–1228 (1997).
25. G. Beheim and K. Fritsch, "Remote displacement measurements using a laser diode," *Electron. Lett.* 21, 93–94 (1983).
26. E. M. Strzelecki, D. A. Cohen, and L. Coldren, "Investigation of tunable single frequency diode lasers for sensor applications," *J. Lightwave Technol.* LT-6, 1610–1680 (1988).
27. A. R. Slotwinski, F. E. Goodwin, and D. L. Simonson, "Utilizing

- AlGaAs laser diodes as a source for frequency modulated continuous wave (FMCW) coherent laser radars," *Proc. SPIE* **1043**, 245–251 (1989).
28. E. C. Burrows and K.-Y. Liou, "High-resolution laser LIDAR utilizing two-section distributed feedback semiconductor laser as a coherent source," *Electron. Lett.* **26**, 577–579 (1990).
 29. A. Dieckmann, "FMCW-LIDAR with tunable twin-guide laser diode," *Electron. Lett.* **30**, 308–309 (1994).
 30. A. Dieckmann and M.-C. Amann, "Phase-noise-limited accuracy of distance measurements in a frequency-modulated continuous-wave LIDAR with a tunable twin-guide laser diode," *Opt. Eng.* **34**, 896–903 (1995).
 31. K. Iiyama, L.-T. Wang, and K. Hayashi, "Linearizing optical frequency-sweep of a laser diode for FMCW reflectometry," *J. Lightwave Technol.* **14**, 173–178 (1996).
 32. K. Nakamura, T. Hara, M. Yoshida, T. Miyahara, and H. Ito, "Optical frequency domain ranging by a frequency-shifted feedback laser," *IEEE J. Quantum Electron.* **36**, 305–316 (2000).
 33. G. Economou, R. C. Youngquist, and D. E. N. Davies, "Limitations and noise in interferometric systems using frequency ramped single-mode diode lasers," *J. Lightwave Technol.* **4**, 1601–1608 (1986).
 34. M.-C. Amann, "Phase-noise limited resolution of coherent LIDAR using widely tunable laser diodes," *Electron. Lett.* **28**, 1694–1696 (1992).
 35. A. Dieckmann and M.-C. Amann, "FMCW-LIDAR with tunable twin-guide laser diode," in *Trends in Optical Fibre Metrology and Standards*, O. D. D. Soares, Ed., pp. 791–802, Kluwer Academic Publishers, Dordrecht (1995).



Markus-Christian Amann received his Diplom degree in electrical engineering in 1976 and his DrIng degree in 1981, both from the Technical University of Munich. During his thesis work, he studied superluminescent diodes and low-threshold laser diodes and developed the AlGaAs-GaAs metal-clad ridge-waveguide laser. From 1981 to 1994 he was with the Corporate Research Laboratories of the Siemens AG in Munich where he was involved in the re-

search on long-wavelength InGaAsP-InP laser diodes. In 1987 he became the head of a research group working on advanced laser diode structures and integrated optoelectronic devices. In February 1994 he joined the Department of Electrical Engineering at the University of Kassel, establishing a working group for III/V semiconductor electronics and optoelectronics. Since November 1997 he has held the chair of semiconductor technology at the Walter Schottky Institute of the Technical University of Munich, where he is currently engaged in research on tunable laser diodes for the near IR, quantum cascade lasers, long-wavelength vertical-cavity laser diodes and laser diode applications. Amann has authored or coauthored about 120 papers on semiconductor optoelectronics in scientific journals and conference proceedings and books. Together with Jens Buus he recently wrote a book on tunable laser diodes. He is a member of the German Informationstechnische Gesellschaft (ITG), and a senior member of the IEEE Lasers and Electro-Optics Society.

Thierry Bosch: Biography appears with the guest editorial in this issue.



Marc Lescure received the PhD degree in electronic engineering from the University of Toulouse in 1972, and the Doctorat d'Etat in 1985. Since 1972, he has been working at the Electronic Laboratory (ENSEEHT) of the National Polytechnics Institut of Toulouse. From 1972 to 1985, his research included characterization of optoelectronic devices (LED, solar cell, MIS) by frequential method. Since 1986, his teaching/research interests has included design of analog circuits, wireless infrared communications and optoelectronic sensors. He has published two books with A. Dziadowiec on the subject of analog circuits and he is coeditor with Thierry Bosch of *Selected Papers on Laser Distance Measurements* in the SPIE Milestone Series.



Risto Myllylä received his DSc (engineering) degree in electrical engineering from the University of Oulu, Finland, in 1976. He has been an associate professor with the Department of Electrical Engineering, University of Oulu since 1974 and a professor since 1995. From 1977 to 1978, he was a visiting scientist with the University of Stuttgart, Germany. From 1988 to 1995 he was a research professor with the Technical Research Centre of Finland. His research interests include industrial and biomedical instrumentation development, particularly in optical measurements. He has coauthored one book and over 240 papers and patents. Dr. Myllylä is a past president of Finnish Optical Society, a board member of European Optical Society, and a member of SPIE, OSA, IEEE, and EOS.



Marc Rioux is a principal research officer with the Institute for Information Technology at the National Research Council. His present interests are in the development of 3-D digitizing, modeling and display for machine vision, optical dimensional inspection and visual communication in the Visual Information Technology Group. He received his BS degree in engineering physics in 1971 and his MS in physics in 1976, both from Laval University. He worked for 5 years on CO₂ laser development and applications and 2 years on IR holography and joined the National Research Council in 1978 to work on optical sensor research.